

Radiation hardness of the electrical properties of carbon nanotube network field effect transistors under high-energy proton irradiation

Woong-Ki Hong¹, Chongoh Lee¹, Dhriti Nepal¹, Kurt E Geckeler¹,
Kwanwoo Shin² and Takhee Lee¹

¹ Department of Materials Science and Engineering, Gwangju Institute of Science and Technology, Gwangju 500-712, Korea

² Department of Chemistry, Sogang University, Seoul 121-742, Korea

E-mail: kwshin@sogang.ac.kr and tlee@gist.ac.kr

Received 12 September 2006, in final form 10 October 2006

Published 30 October 2006

Online at stacks.iop.org/Nano/17/5675

Abstract

The effect of high-energy proton irradiation on the physical properties of carbon nanotubes (CNTs) was investigated. The focus of the study was on the electrical properties of single-walled carbon nanotube (SWNT) network devices exposed to proton beams. Field-effect transistors (FETs) of network type were fabricated using SWNTs and were then irradiated by high-energy proton beams of 10–35 MeV with a fluence of 4×10^{10} – 4×10^{12} cm⁻² that are comparable to the aerospace radiation environment. The electrical properties of both metallic and semiconducting CNT network FET devices underwent no significant change after the high-energy proton irradiation, indicating that the CNT network devices are very tolerant in proton beams. Raman spectra confirm the proton-radiation hardness of CNT network FET devices. The radiation hardness of CNT network FET devices promises therefore the potential usefulness of CNT-based electronics for future space application.

(Some figures in this article are in colour only in the electronic version)

1. Introduction

Carbon nanotubes (CNTs), having outstanding mechanical properties (i.e., Young's modulus 10³ GPa) with a nanoscale diameter ranging from 3 to 30 nm, are promising materials in a wide range of emerging technologies. In particular, due to their unique electrical properties, various potential applications in nanoelectronics, such as nanotube field-effect transistors (FETs), CNT-based nonvolatile memory, quantum-effect devices, and sensors, are currently being developed [1–4].

The electrical properties of CNTs are strongly dependent on their atomic structures: a nanotube can be metallic or semiconducting depending on the chirality vector (n, m) that defines the diameter and the chiral angle of a CNT [2]. Furthermore, the electrical properties of CNTs are extremely

sensitive to defects which can be introduced during the growth, by mechanical strain, or by irradiation with energetic particles such as electrons, heavy ions, alpha-particles, and protons. Recently, the effects of electron and heavy-ion irradiation on CNTs have been reported [5–7]. A controlled irradiation on CNTs might be a method for modifying the physical and chemical properties of CNTs by introducing structural defects into the side walls. On the other hand, when highly energetic particles collide, a latchup, electrical interference, charging, sputtering, erosion, and puncture of the target device can occur. As a result, degradation of the device performance and lifetime or even a system failure of the underlying electronics may happen. Consequently, information on the effects of various types of irradiation on CNTs is needed in developing radiation-robust devices and circuits for CNT-based devices in aerospace radiation environments.

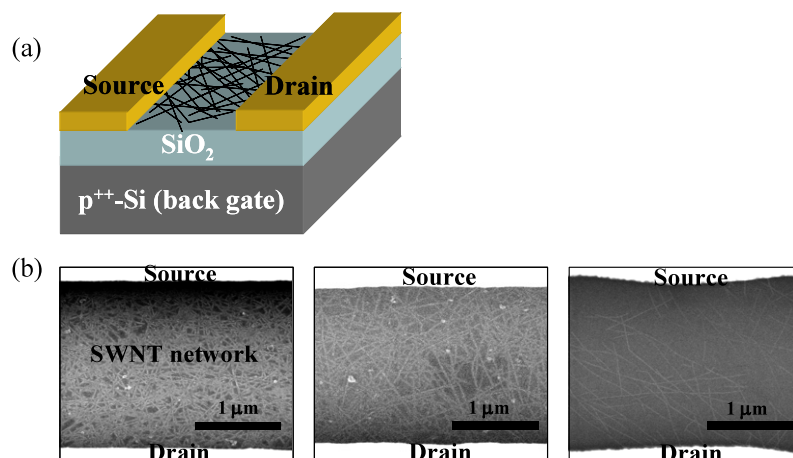


Figure 1. (a) Schematic drawing of single-walled carbon nanotube network field effect transistor (SWNT network FET). (b) SEM images of SWNT network FETs showing different densities of SWNTs connected between the source and drain electrodes.

The radiation environment in the Earth's magnetosphere consists of a nearly isotropic flux of energetic charged particles: 85% protons, 14% alpha-particles, and 1% heavy ions covering the full range of elements [8, 9]. Such radiation may impinge on devices and circuits, causing undesirable effects as described above. Among the various kinds of radiation sources, protons comprise an important component in the radiation belts around the Earth.

Many studies on the effects of proton irradiation on silicon-based devices [10, 11], solar cells [12, 13], GaAs systems [14, 15], and GaN systems [16, 17] have been reported. In particular, Srour and McGarrity [18] reviewed the effects of radiation and damage mechanisms in some of the most commonly employed device materials such as Si, SiO₂, and GaAs, as well as silicon MOS devices, GaAs devices, optoelectronic devices, etc. However, as regards the effects of proton irradiation on CNTs, to date, only a few studies, involving CNTs/polymer composites [19], CNTs films [20], and CNTs predeposited on TEM grids [21] under proton irradiation, have been reported. For example, Neupane *et al* [19] reported that proton irradiation (beam energy = 2 MeV, fluence = 5.0×10^{10} – 5.6×10^{15} cm⁻²) had little effect on the interband transitions in SWNTs matrixed in poly(3-octylthiophene) polymer with small radiation-related degradation. Khare *et al* [20] reported that the C–H bonds were formed in 0.5 and 16.75 μm thick SWNT films upon a high-dose proton irradiation (beam energy = 1 MeV, fluence = 10^{14} cm⁻²). And Basiuk *et al* [21] showed that the morphologies of SWNTs deposited on TEM grids changed with 3 MeV proton irradiation. The question as to whether these radiation-induced effects (related to structural properties) of CNTs are critical to device performances (related to electrical properties) has not yet been directly answered. In order to address this issue regarding the electrical properties in CNT-based devices we must first test the influences of proton irradiation on real device systems. CNT-based FET devices, in which the source–drain currents and gate voltages can be determined, can thus be used to investigate the proton radiation effects on CNTs without being altered by a further chemical process.

In this paper, we report on a systematic study of the effects of proton irradiation on the electrical properties of CNT network FET devices showing metallic or semiconducting behaviours. The CNT-FET devices were exposed to 10–35 MeV proton beams with a fluence of 4×10^{10} – 4×10^{12} cm⁻² that are comparable to the aerospace environment. We also performed micro-Raman spectroscopy directly on the CNT-FET devices to correlate the structural changes to any potential electrical property changes in CNTs under proton irradiation. Proton implant effects were modelled using SRIM-2003 (stopping and range of ions into matter) [22].

2. Experimental details

We fabricated the CNT network FET devices using single-walled carbon nanotubes (SWNTs) by an arc-discharge process (commercially available from Iljin Nanotech Co., Ltd, Korea). The SWNTs were purified to ~95% by thermal oxidation and chemical treatment. To fabricate CNT network FET devices, SWNTs in 1,2-dichlorobenzene (*o*-DCB) (from Sigma-Aldrich) were prepared by a combination of sonication and centrifugation. In a typical experiment, 1 mg of SWNT in 10 ml of *o*-DCB was sonicated for 5 min and the SWNT suspension was then centrifuged for 90 min at 16 000 g. The purified SWNTs suspension was dropped on a 100 nm or a 300 nm thick thermally grown oxide on silicon. The silicon substrate was a highly doped p-type substrate that can be used as a back gate. The SWNTs dropped on the substrates were dried in a vacuum oven overnight above 180 °C, to remove *o*-DCB chemical residue. Metal electrodes consisting of Ti (30 nm)/Au (60 nm) were then deposited by an electron-beam evaporator and defined as the source and drain electrodes by photolithography and a lift-off process. The distance between the source and drain electrodes was 2–3 μm. A schematic diagram of a fabricated SWNT network FET device is shown in figure 1(a).

For the proton irradiation experiments, accelerated proton beams were generated using a MC-50 cyclotron (at the Korea Institute of Radiological and Medical Sciences). The beam diameter was ~6 cm, its uniformity was ~90%, and the

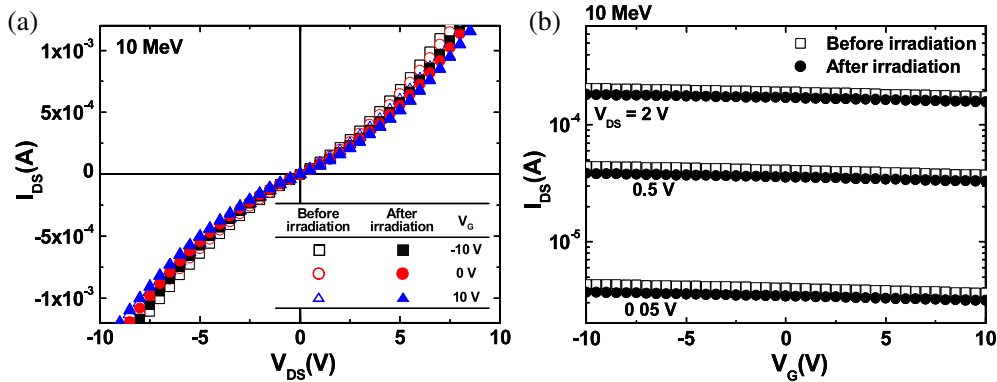


Figure 2. Transfer characteristics of metallic SWNT network FETs before and after proton irradiation at 10 MeV and a fluence of $1.4 \times 10^{12} \text{ cm}^{-2}$. (a) Source–drain current versus drain voltage at various gate voltages ($V_G = -10, 0,$ and 10 V). (b) Source–drain current as a function of gate voltage at various source–drain biases ($V_{DS} = 0.05, 0.5,$ and 2 V).

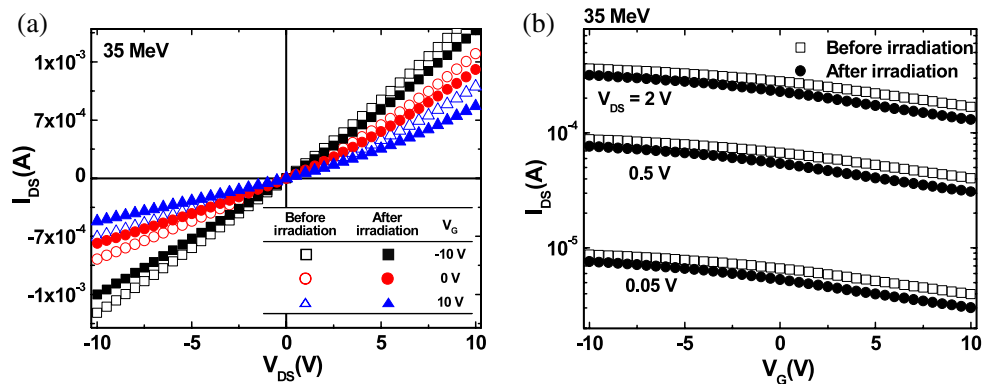


Figure 3. Transfer characteristics of weak-metallic SWNT network FETs before and after proton irradiation at 35 MeV and a fluence of $4.1 \times 10^{11} \text{ cm}^{-2}$. (a) Source–drain current versus drain voltage at various gate voltages ($V_G = -10, 0,$ and 10 V). (b) Source–drain current as a function of gate voltage at various source–drain biases ($V_{DS} = 0.05, 0.5,$ and 2 V).

average beam current was 10 nA. In our study, three different proton beam energies were used: 10, 20, and 35 MeV. The total fluences during the proton irradiation were 1.2×10^{11} – $1.4 \times 10^{12} \text{ cm}^{-2}$ for 10 and 20 MeV and 4.1×10^{10} – 4.1×10^{12} for 35 MeV. In particular, for the proton irradiation of 35 MeV, we used the spread-out Bragg peak (SOBP) method. The SOBP method is a range-modulating method to obtain a uniform longitudinal and transverse dose distribution in a target for a fixed proton energy [23]. The irradiation time of the proton beams was varied from 60 to 6000 s. Actually, the 30–60 MeV protons at a dose of $\sim 10^{12} \text{ cm}^{-2}$ are equivalent to an amount of proton radiation for a few hundred years in a low Earth orbit environment [24].

Electrical properties such as source–drain current–voltage characteristics as a function of gate voltage were measured using a HP4155C semiconductor parameter analyser. The gate voltage was applied through the highly doped silicon back gate. Raman analysis was also performed to collect the information on structural defects that might be introduced by proton irradiation using a Renishaw (System 2000) micro-Raman spectrometer in the backscattering configuration. A 633 nm He–Ne laser was used for excitation in this case. For the simulation of the depth profile of proton reaction with our device materials, we used the SRIM simulator, a numerical code based on a Monte Carlo simulation, assuming a carbon

density of 2.26 g cm^{-3} (to provide a projected range and stopping power) [22].

3. Results and discussion

Figure 1(b) shows scanning electron microscope (SEM) images of three representative SWNT network FET devices showing different density of SWNTs connected between the source and drain electrodes with a $2\text{--}3 \mu\text{m}$ gap. The different density is responsible for different electrical properties: metallic, weak-metallic, or semiconducting behaviours. As explained later, the SEM images from left (high density of CNTs) to right (low density of CNTs) correspond to metallic, weak-metallic, and semiconducting type CNT network FET devices, respectively.

Figures 2 and 3 show representative data for the SWNT network FET devices, which show metallic or weak-metallic (weak-semiconducting) behaviours before and after proton irradiation. These figures are the transfer characteristics of an SWNT network FET device before and after proton irradiation at 10 and 35 MeV, respectively. The irradiation time and the fluence for the devices shown in figures 2 and 3 were 1800 and 600 s, 6.9×10^{11} and $4.1 \times 10^{11} \text{ cm}^{-2}$ for 10 and 35 MeV, respectively.

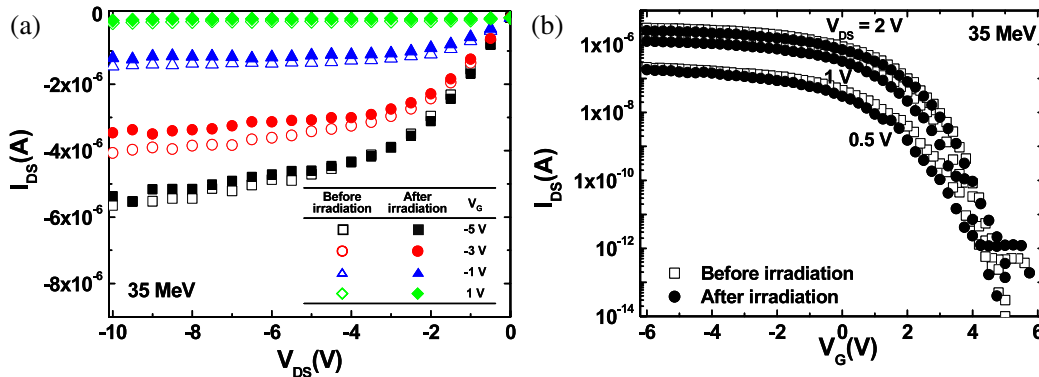


Figure 4. Transfer characteristics of semiconducting SWNT network FETs before and after proton irradiation with energy of 35 MeV and fluence of $4.1 \times 10^{12} \text{ cm}^{-2}$. (a) Source–drain current versus drain voltage at various gate voltages ($V_G = -5, -3, -1, \text{ and } 1 \text{ V}$). (b) Source–drain current as a function of gate voltage at various source–drain biases ($V_{DS} = 0.5, 1, \text{ and } 2 \text{ V}$).

We first measured the transfer characteristics before proton irradiation followed by exposure of the device to the proton beam, and then measured the characteristics of the same device after proton irradiation. Figures 2(a) and 3(a) show the source–drain current versus voltage (I_{DS} – V_{DS}) characteristics for different gate voltages and figures 2(b) and 3(b) show the source–drain current versus gate voltage (I_{DS} – V_G) characteristics for different source–drain biases. The nearly ohmic shape and negligible dependence on the gate voltage indicate that these SWNT network FET devices behave in a metallic (figure 2) or weak-metallic (slight semiconducting) manner (figure 3). Although the current level was reduced slightly (by less than $\sim 2\%$) after the proton irradiation as compared with that before the irradiation, the basic transfer characteristics were not influenced by proton irradiation. Similarly, devices exposed to proton beams of 20 MeV (not shown here) also exhibited a negligible response after proton irradiation.

We also investigated the electrical properties of SWNT network FET devices showing semiconducting behaviour and representative data are shown in figure 4. These particular devices show p-type semiconducting behaviour, since the current increases with increasing negative gate voltage whereas it decreases down to a few picoamperes (pA) with increasing positive gate voltage. The p-type behaviour of SWNTs has been attributed to the adsorbed oxygen from the ambient air [25]. The ratio of the current change (I_{on}/I_{off}) is over 10^5 at $V_{DS} = 0.5 \text{ V}$ while the gate voltage was swept from -6 to 6 V . Similarly to the metallic and weak-metallic SWNT network FET devices (figures 2 and 3), the electrical transport properties of the semiconducting SWNT network FET are also not influenced by the proton irradiation (figure 4). The irradiation conditions for this particular device were beam energy = 35 MeV, irradiation time = 6000 s, and proton fluence = $4.1 \times 10^{12} \text{ cm}^{-2}$.

It is noted that the network SWNT-FETs showed either metallic (figure 2; left SEM image in figure 1(b)), weak-metallic (figure 3; middle SEM image in figure 1(b)), or semiconducting (figure 4; right SEM image in figure 1(b)) nature, which can be attributed to the difference of nanotube density in the network. Snow *et al* [26] investigated a random network of SWNTs based on the density of nanotubes.

Table 1. The experimental conditions for proton irradiation.

Energy (MeV)	Irradiation time (s)	Fluence ($\# \text{ cm}^{-2}$)
10, 20	300	1.2×10^{11}
	600	2.3×10^{11}
	1800	6.9×10^{11}
	3600	1.4×10^{12}
35 (SOBP) ^a	60	4.1×10^{10}
	600	4.1×10^{11}
	6000	4.1×10^{12}

^a SOBP (spread-out Bragg peak) is a range-modulating method to obtain a uniform dose distribution in a target [23].

They have found that an SWNT network with a low density behaves like a p-type semiconductor and an SWNT network becomes metallic if the density of metallic nanotubes exceeds a percolation threshold.

In our study, as summarized in table 1, we have varied the proton irradiation conditions: beam energy of 10–35 MeV, an irradiation time of 60–6000 s, and a proton fluence of 4×10^{10} – $4 \times 10^{12} \text{ cm}^{-2}$, which are comparable to aerospace environments. Although not all of the results for the SWNT network FET devices are presented here, none of the SWNT network FET devices (26 devices) systematically measured exhibited any significantly altered electrical changes before and after proton irradiation. These results indicate a certain radiation hardness of CNT-based electronic devices under proton irradiation in our exposure conditions and suggest that the CNT devices are promising for future application in aerospace. Our results are consistent with the report by Neupane *et al* [19] that CNT/polymer composites exposed to the proton beams were very radiation tolerant, with the potential to be durable in space applications.

Since the electrical properties are strongly related to molecular arrangements, for example, the bandgap is inversely related to tube diameter, the lattice information of CNTs should be cross-checked to see whether the radiation might influence their geometrical structures. We performed Raman spectroscopy to investigate potential structural modifications which might occur during proton irradiation in our SWNT network FET devices. A 632.8 nm He–Ne laser (50 mW)

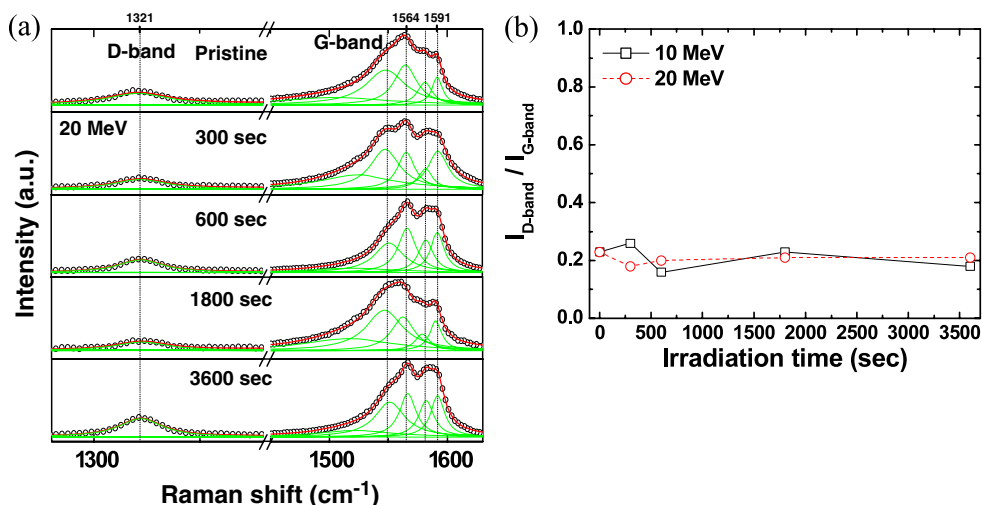


Figure 5. (a) Raman spectra at an excitation wavelength of 633 nm for the SWNT network FETs before (pristine) and after proton irradiation of 20 MeV for 300, 600, 1800, and 3600 s corresponding to the fluence of 1.2×10^{11} , 2.4×10^{11} , 6.9×10^{11} , and $1.4 \times 10^{12} \text{ cm}^{-2}$, respectively. (b) The intensity ratio of D-band to G-band at different radiation time periods for 10 and 20 MeV proton beams.

was directly focused on the SWNT network in the CNT-FET devices at room temperature. We focused on the disorder-induced mode (D-band) and tangential modes (G-band) in the $1200\text{--}1700 \text{ cm}^{-1}$ region, which are activated in the first-order scattering process of sp^2 carbons by the presence of in-plane substituted hetero-atoms, vacancies, grain boundaries or other defects caused by the proton irradiation, and related to a well-ordered graphite, respectively. Figure 5(a) shows Raman spectra (circular symbols) between 1200 and 1700 cm^{-1} for an unirradiated device (pristine) and a series of proton (20 MeV)-irradiated SWNT network FET devices for various time periods. A disorder-induced D-band at $\sim 1321 \text{ cm}^{-1}$ is clearly observed. The tangential (G-band) Raman feature with multi-peaks around $1500\text{--}1600 \text{ cm}^{-1}$ is due to the vibration symmetry of the SWNTs [27] and can be decomposed into four Lorentzian curves (four solid curves): 1548 , 1564 , 1581 , and 1591 cm^{-1} peaks. The broad peak around 1520 cm^{-1} is the Breit–Wigner–Fano (BWF) line due to the presence of metallic nanotubes, and the region of the BWF line can be changed by aggregation and bundling of nanotubes [28]. The peak around 1581 cm^{-1} is observed in many graphite-like materials with a metallic character, such as n-doped graphite intercalation compounds and n-doped fullerenes as well as metallic SWNTs [28, 29]. It can be seen that, although the Raman spectra are not exactly the same before and after proton irradiation, the peak positions of D-band peak (1321 cm^{-1}) and G-band peaks (1548 , 1564 , 1581 , 1591 cm^{-1}) for the proton-irradiated devices do not change with respect to those for the unirradiated (pristine) device (figure 5(a)), indicative of insignificant modification of the band gap structure [30]. Furthermore, in order to see if any significant defects were produced by the proton irradiations, the intensity ratio ($I_{\text{D-band}}/I_{\text{G-band}}$) of D-band to G-band in the Raman spectra were then compared. As shown in figure 5(b), the intensity ratios ($I_{\text{D-band}}/I_{\text{G-band}}$) did not change significantly with irradiation time for 10 and 20 MeV proton beams. These results suggest the proton irradiation did not influence the structures of the SWNTs and thus support

the irradiation hardness of the electrical properties of SNWT network FET devices (figures 2–4).

To understand the proton radiation hardness of our CNT-FET devices, we studied the depth profile of proton reaction with our device materials using a simulation of the Monte Carlo code SRIM-2003 [22]. For the simulations, we assumed that the density of the SWNT network is 2.26 g cm^{-3} (carbon) and followed a procedure in the SRIM calculation for protons, described in [31]. The projected ranges for the proton beams of $10\text{--}35 \text{ MeV}$ were determined and were found to be around $500\text{--}5000 \mu\text{m}$ deep into the material. Khare *et al* [20] reported that, according to Monte Carlo simulations, 1 MeV protons implant into carbon materials mostly at distances of $16\text{--}18 \mu\text{m}$. The thickness of the SWNT network in our device structure is thin (a few nm), which is very small compared to the depth of penetration of proton beams of $10\text{--}35 \text{ MeV}$ (500 to $5000 \mu\text{m}$). The accelerated proton particles deposit their energy near the end of their path (called a Bragg peak) and the proton beams used in our experiment do not decrease (up to a few μm deep) from the SRIM simulation, which indicates that the proton beam simply penetrates through the SWNT layer in our device structure without losing its energy.

It has been reported that electronic devices became more radiation tolerant when their dimensions are reduced [32, 33]. For example, multi-quantum well or quantum dot devices can be tens or hundreds times more radiation tolerant than conventional bulk devices [32]. Weaver *et al* [33] even reported that quantum dot/CNT-based photovoltaic devices were five orders of magnitude more resistant than conventional bulk solar cells. These results agree with our observation that the CNT network FET devices fabricated in our study are very tolerant to high-energy proton irradiation of $10\text{--}35 \text{ MeV}$ with a fluence of $4 \times 10^{10}\text{--}4 \times 10^{12} \text{ cm}^{-2}$.

4. Conclusion

In summary, we fabricated FETs of a network type using SWNTs and examined the electrical properties of CNT network FET devices before and after high-energy proton

irradiation. From electrical measurement and Raman spectra, we found that the electrical properties of SWNT network FET devices undergo no significant changes as the result of proton irradiation with an energy of 10–35 MeV and a fluence of 4×10^{10} – 4×10^{12} cm⁻². The electrical results and Raman data indicate that CNT network FET devices are very tolerant under our proton beam conditions which are comparable to an aerospace environment, and suggest a radiation hardness of CNT-related electronic devices when used in outer space.

Acknowledgments

This research work was financially supported by the Development and Management of Proton Accelerator User Program, as a part of the 21st Century Frontier R&D Program supported by the Ministry of Science and Technology and the Basic Research Program of the Korea Science and Engineering Foundation (Grant No. R01-2005-000-10815-0).

References

- [1] Iijima S 1991 *Nature* **354** 56
- [2] Avoris Ph, Appenzeller J, Matel R and Wind S J 2003 *Proc. IEEE* **91** 1772
- [3] Dresselhaus M S, Dresselhaus G and Avouris Ph 2001 *Carbon Nanotubes: Synthesis, Structure properties and Applications* (Berlin: Springer)
- [4] Choi W B, Bae E, Kang D, Chae S, Cheong B, Ko J, Lee E and Park W 2004 *Nanotechnology* **15** S512
- [5] Krasheninnikov A V, Nordlund K, Sirviö M, Salonen E and Keinonen J 2001 *Phys. Rev. B* **63** 245405
- [6] Ni B, Andrews R, Jacques D, Qian D, Wijesundara M B J, Choi Y, Hanley L and Sinnott S B 2001 *J. Phys. Chem. B* **105** 12719
- [7] Stahl H, Appenzeller J, Martel R, Avouris Ph and Lengeler B 2000 *Phys. Rev. Lett.* **85** 5186
- [8] Khanna R *et al* 2004 *J. Electron. Mater.* **34** 395
- [9] Holmes-Siedle A and Adams L 1993 *Handbook of Radiation Effects* (Oxford: Oxford University Press)
- [10] Ohyama H, Hayama K, Vanhellenmont J, Poortmans J, Caymax M, Takami Y, Sunaga H, Nahiyama I and Uwatoko Y 1996 *Appl. Phys. Lett.* **69** 2429
- [11] Siad M, Keffous A, Belkacem Y, Menari H, Mamma S and Chaouch C L 2003 *Nucl. Instrum. Methods Phys. Res. A* **512** 106
- [12] Rong W, Zengliang G, Xinghui Z and Zuoxu Z 2003 *Sol. Energy Mater. Sol. Cells* **77** 351
- [13] Jasenek A and Rau U 2001 *J. Appl. Phys.* **90** 650
- [14] Dharmarasu N, Arulkumaran S, Sumathi R R, Jayavel P, Kumar J, Magudapathy P and Nair K G M 1998 *Nucl. Instrum. Methods Phys. Res. B* **140** 119
- [15] Luo B, Johnson J W, Ren F, Allums K K, Abernathy C R, Pearton S J, Dwivedi R, Fogarty T N and Wilkins R 2002 *J. Electrochem. Soc.* **149** G236
- [16] Hu X, Karmarkar A P, Fleetwood D M, Schrimpf R D, Geil R D, Weller R A, White B D, Bataiev M, Brillson L J and Mishra U K 2003 *IEEE Trans. Nucl. Sci.* **50** 1791
- [17] Luo B *et al* 2003 *Solid-State Electron.* **47** 1015
- [18] Srouf J R and McGarrity J M 1988 *Proc. IEEE* **76** 1443
- [19] Neupane P P, Manasreh M O, Weaver B D, Raffaella R P and Landi B J 2005 *Appl. Phys. Lett.* **86** 221908
- [20] Khare B, Meyyappan M, Moore M H, Wilhite P, Imanaka H and Chen B 2003 *Nano Lett.* **3** 643
- [21] Basiuk V A, Kobayashi K, Kaneko T, Negishi Y, Basiuk E V and Saniger-Blesa J M 2002 *Nano Lett.* **2** 789
- [22] Ziegler J F, Biersack J P and Littmarck U 1995 *Stopping and Range of Ions into Matter* (New York: Pergamon)
- [23] Lim Y K, Park B S, Lee S K and Kim K R 2006 *J. Kor. Phys. Soc.* **48** 777
- [24] Metayer P Le, Gilard O, Germanicus R, Campillo D, Ledu F, Cazes J, Falo W and Chatry C 2003 *J. Appl. Phys.* **94** 7757
- [25] Kang D, Park N, Ko J, Bae E and Park W 2005 *Nanotechnology* **16** 1048
- [26] Snow E S, Novak J P, Campbell P M and Park D 2003 *Appl. Phys. Lett.* **82** 2145
- [27] Jorio A, Dresselhaus G, Dresselhaus M S, Souza M, Dantas M S S, Pimenta M A, Rao A M, Saito R, Liu C and Cheng H M 2000 *Phys. Rev. Lett.* **85** 2617
- [28] Heller D A, Barone P W, Swanson J P, Mayrhofer R M and Strano M S 2004 *J. Phys. Chem. B* **108** 6905
- [29] Jorio A, Pimenta M A, Souza Filho A G, Saito R, Dresselhaus G and Dresselhaus M S 2003 *New J. Phys.* **5** 139
- [30] Dresselhaus M S, Dresselhaus G, Saito R and Jorio A 2005 *Phys. Rep.* **409** 47
- [31] Messenger S R, Burke E A, Summer G P and Xapsos M A 1999 *IEEE Trans. Nucl. Sci.* **46** 1595
- [32] Weaver B D 2005 New dimensions in radiation effects *electronics and electromagnetics in 2005 NRL Rev.*
- [33] Weaver B D, Landi B J and Raffaella R P 2004 High radiation tolerance of carbon nanotube matrices for space power applications *2nd Int. Energy Conversion Engineering Conf.*